J Biosci (2021)46:72
DOI: 10.1007/s12038-021-00187-x

Review

Metastable biomolecular condensates of interferon-inducible antiviral Mx-family GTPases: A paradigm shift in the last three years

PRAVIN B SEHGAL

Departments of Cell Biology and Anatomy, and Medicine, New York Medical College, Valhalla, NY, USA

(Email, pravin_sehgal@nymc.edu)

MS received 17 December 2020; accepted 5 June 2021

Membraneless organelles (MLOs) in the cytoplasm and nucleus in the form of phase-separated biomolecular condensates are increasingly viewed as critical in regulating diverse cellular functions. We summarize a paradigm shift over the last 3 years in the field of interferon (IFN)-inducible antiviral Mx-family GTPases. Expression of the 'myxovirus resistance proteins' MxA in human cells and its ortholog Mx1 in murine cells is increased 50- to 100-fold by Type I (IFN-α and -β) and III IFNs (IFN-λ). Human MxA forms *cytoplasmic* structures, while murine Mx1 forms *nuclear* bodies. Since 2002, it has been widely thought that human (Hu) MxA is associated with the membraneous smooth endoplasmic reticulum (ER). In a paradigm shift, our recent data showed that HuMxA formed membraneless phase-separated biomolecular condensates in the cytoplasm. Some of the HuMxA condensates adhered to intermediate filaments generating a reticular pattern. Murine (Mu) Mx1, which was predominantly nuclear, was also confirmed to be in phase-separated nuclear biomolecular condensates. A subset of Huh7 cells showed association of GFP-MuMx1 with intermediate filaments in the cytoplasm. While cells with cytoplasmic GFP-HuMxA condensates and cytoplasmic GFP-MuMx1 filaments showed an antiviral phenotype towards vesicular stomatitis virus (VSV), those with only nuclear GFP-MuMx1 bodies did not. The new data bring forward the paradigm that both human MxA and murine Mx1 give rise to phase-separated biomolecular condensates, albeit in different subcellular compartments, and that differences in the subcellular localization of condensates of different Mx proteins determines the spectrum of their antiviral activity.

Keywords. Interferons; myxovirus resistance proteins; cytoplasmic human MxA condensates; nuclear and cytoplasmic murine Mx1 condensates; subcellular localization; antiviral activity; tonicity- and crowding-driven metastability

1. Introduction

In the process of investigating a phenomenon called 'viral interference' in which one virus interferes with the replication of another related or even unrelated virus, Isaacs and Lindenmann observed in 1957 that chicken embryo tissue in cell culture exposed to live or ultraviolet-irradiated influenza virus type A (FLUAV, an RNA-containing myxovirus isolated from humans) secreted a protein into the culture medium which could render fresh cultures of chicken tissue resistant to a challenge with live FLUAV (Isaacs and Lindenmann 1957; Isaacs *et al.* 1957). This protein, which elicited an antiviral effect against FLUAV, was called 'interferon' (IFN). Subsequently, Lindenmann investigated human-derived FLUAV strain adapted to mice and observed that while the A2G strain of inbred mice, and outbred and field mice were resistant to the production of pulmonary disease when FLUAV was administered

This article is dedicated to the memory of the late Dr. Manohar V. Shirodkar, Director, The Haffkine Institute, Mumbai, India, who taught the author to go wherever the data led.

Published online: 29 July 2021

by inhalation, other inbred mouse strains (e.g. Balb/c) were susceptible (Lindenmann 1962; Lindenmann *et al.* 1963). It was soon recognized that this resistance to inhaled FLUAV was due to a genetic trait dubbed '*Mx*' for 'myxovirus resistance gene.' (Lindenmann *et al.* 1963; Lindenmann 1964; Haller *et al.* 2015, 2018).

Contemporaneously with these studies, numerous investigators examined the ability of one virus to inhibit development of disease by other disparate viruses in animal models (Henle 1950; Ho 1962). One such investigation, initiated in the early 1960s at the Johns Hopkins School of Public Health and continued at the Virus Research Center, Pune (now called the National Institute of Virology) showed that West Nile virus inoculation of chicken could block the development of sarcoma in the wing web following a challenge with the Rous sarcoma virus (Shirodkar 1965). Subsequently it was discovered that a vaccine strain of rabies virus was also able to cause this blockade of the Rous sarcoma in chicken (Desai 1970), and that the plasma/serum of rabies virus-inoculated chicken contained a protein which blocked sarcoma development produced by the Rous virus (Desai *et al.* 1973). Taken together, an interpretation of these observations was the possibility that virus-induced interferon mediated this anti-tumor effect (Shirodkar 1965; Desai 1970; Desai *et al.* 1973). Parenthetically, the present author received his first detailed education about the interferons through participation with Dr. M. V. N. Shirodkar in some of these studies (Desai *et al.* 1973).

Evidence for the involvement of interferon (IFN) *in vivo* in mice resistant to an inhaled challenge of FLUAV was reported in 1979 by Haller and colleagues (as part of the Lindenmann research group) (Haller *et al.* 1979). An antibody that neutralized mouse IFN administered to A2G mice rendered such resistant mice susceptible to development of viral pneumonia. Thus, the '*Mx*' resistance gene produced an IFN-inducible gene product with antiviral activity against FLUAV and other myxo- and paramyxoviruses. Over the next two decades, in very elegant studies, Haller and colleagues, identified the mouse Mx1 and as well as human MxA proteins as 60–70 kDa dynamin-family large GTPases which had an antiviral effect against a variety of different RNA- and DNA-containing viruses (table 1; Verhelst *et al.* 2013; Haller *et al.* 2015 2018). Exposure to cells with appropriate IFN preparations upregulated Mx RNA and protein expression by 50- to 100-fold in human and mouse cells (Haller *et al.* 2015 2018; Yuan and Sehgal 2016). Moreover, a second human Mx gene ('*MxB*') was discovered, as was a second mouse Mx gene ('*Mx2*') (Haller *et al.* 2015, 2018). Phylogenetic analyses showed that *MxA* and *MxB* represented distinct genes, but that murine *Mx1* and *Mx2* were orthologs of *MxA* (the rodent ortholog of *MxB* had been lost) (table 1; Busnadiego *et al.* 2014; Haller *et al.* 2015). Human MxA and MxB, and murine Mx1 and Mx2 proteins had distinct subcellular localizations (cytoplasmic vs. nuclear) and distinct antiviral activities towards different viruses (table 1; see Verhelst *et al.* 2013; Haller *et al.* 2015, 2018, Steiner and Pavlovic 2020 for detailed reviews).

Briefly, human MxA formed cytoplasmic structures, human MxB was located in structures near the nuclear pores, murine Mx1 formed nuclear structures, while murine Mx2 was 'granular' and in the cytoplasm. Additionally, human MxA was antiviral towards FLUAV and vesicular stomatitis virus (VSV, a rhabdovirus whose entire life cycle is cytoplasmic), while human MxB was antiviral towards lentiviruses such as HIV but not FLUAV or VSV. In contrast to human MxA, the orthologous nuclear murine Mx1 was antiviral towards FLUAV (which has an obligatory nuclear step in its life cycle) but not against VSV, while, curiously, the cytoplasmic granular murine Mx2 (also an ortholog of human MxA) was antiviral towards VSV (Haller *et al.* 2015; Sehgal *et al.* 2020b) (table 1). The GTPase activity was required for these antiviral activities (Dick *et al.* 2015; Nigg and Pavlovic 2015; Haller *et al.* 2015, 2018). However, despite extensive studies over the last six decades, the molecular mechanisms by which Mx proteins inhibit replication of different viruses in intact cells are incompletely understood (Haller *et al.* 2015, 2018; Sehgal *et al.* 2020b; Steiner and Pavlovic 2020). Surprisingly, even the understanding of the basic cell biology of Mx proteins needed a paradigm shift in the last three years.

2. A paradigm shift in the Mx field in last three years

In 2002 the Haller group (Kochs *et al.* 2002) reported that electron microscopy of cells transfected with human MxA expression vector together with infection by La Crosse virus revealed juxtanuclear *membrane-less* structures which contained the viral nucleocapsid (N) protein and MxA. In this article in 2002, Haller and colleagues stated specifically that these structures did not associate with any intracellular membranes (Kochs *et al.* 2002).

Table 1. Condensates of different human and murine Mx proteins

Protein	Cellular localization	Illustrative Antiviral activity*	References
Human MxA	Cytoplasmic condensates with some tethered to intermediate filaments	vs. both FLUAV and VSV	Davis *et al.* (2018, 2019)
Human MxB (full length)	Cytoplasmic face of nuclear pores,	vs. HIV; not vs. FLUAV nor VSV	King *et al.* (2004)
	Cytoplasmic condensates		Goujon *et al.* (2013) our inference
Murine Mx1	nuclear condensates	vs. FLUAV; not VSV	Sehgal *et al.* (2020b)
	cytoplasmic intermediate filaments and condensates	vs. VSV	Sehgal *et al.* (2020b)
Murine Mx2	Cytoplasmic structures	vs. VSV; not FLUAV	Haller *et al.* (2015)

*See reviews Verhelst *et al.* (2013), Haller *et al.* (2015, 2018) and Steiner and Pavlovic (2020) for detailed antiviral spectrum reported in the previous literature.

Modified from Sehgal *et al.* (2020b).

In contrast, also in 2002, McNevin and colleagues (Accola *et al.* 2002) claimed that MxA expressed in Hela and Hep3B cells was associated with the smooth endoplasmic reticulum (ER). However, in the article itself, these authors admitted that they were unable to associate MxA with any customary markers for the ER or any other membrane-bound organelles, and that the association was 'presumed' to be with the ER because of an impression that MxA colocalized with the 'autocrine motility factor receptor' (AMF), which they claimed had been assigned by them to the ER. Nevertheless, the abstract dropped the 'presumably' and the title of Accola *et al.* (2002) stated categorically that MxA was associated with the smooth ER.

In 2006, Haller and colleagues (Stertz *et al.* 2006) appear to have adjusted their earlier inference from 2002 that MxA structures were membraneless (as in Kochs *et al.* 2002) and now claimed that MxA associated with a 'distinct subcompartment of the smooth endoplasmic reticulum' in the cells they now investigated (the Huh7 human hepatoma cell line) (Stertz *et al.* 2006). Experimentally, Stertz *et al.* (2006) showed images of Huh7 cells with a cytoplasmic resticular meshwork distribution of HA-MxA. The customary markers for ER were of no avail, but an in-house antibody towards syntaxin 17 was presented as a marker of the ER (see figure 3 below for the correct answer: that meshwork in Huh7 cells is of HA-MxA condensates adhering to intermediate filaments; Davis *et al.* 2019; Sehgal *et al.* 2020a).

The two articles – Accola *et al.* (2002) and Stertz *et al.* (2006) – have had a strong grip on the MxA field despite the inconclusive data presented. Hundreds of citations have referred to these two articles as evidence that MxA associates with smooth endoplasmic reticulum. Even the Kochs *et al.* (2002) article which showed 'membraneless' structures of MxA is repetitively misquoted in the Mx literature as having shown that MxA associates with the ER (see Sadler and Williams 2011 for one example).

Against this cumulative backdrop in the MxA field over the last 15 years, the author's lab stumbled on to observations that did not fit with the ER localization of MxA (Yuan and Sehgal 2016). Figure 1A shows examples of variably shaped and sized mesoscale structures in the cytoplasm of HEK293T cells expressing HA-MxA (using the expression construct provided by Stertz *et al.* 2006). Figure 1B shows that at higher magnification the HA-MxA structures were clearly distinct from the reticulon-4-containing endoplasmic reticulum (Yuan and Sehgal 2016; Davis *et al.* 2019). Numerous additional studies in the author's lab showed the divergence of MxA structures from the ER (summarized in Davis, *et al.* 2018; 2019). Thus, by the fall of 2016, we had concluded that there was little convincing experimental evidence that MxA associated with the ER. However, the paradigm in the field that 'MxA associates with the ER' based on Accola *et al.* (2002) and Stertz *et al.* (2006), was overwhelmingly and vigorously espoused (especially by numerous reviewers).

The formal observation by us in Dec 2017 using correlated light and electron microscopy (CLEM) methods that GFP-MxA structures in Huh7 cells were membraneless strengthened our inference ('MxA structures are not ER') (Davis *et al.* 2018 2019) (figure 2). These membraneless structures were associated with an extensive meshwork of intermediate filaments

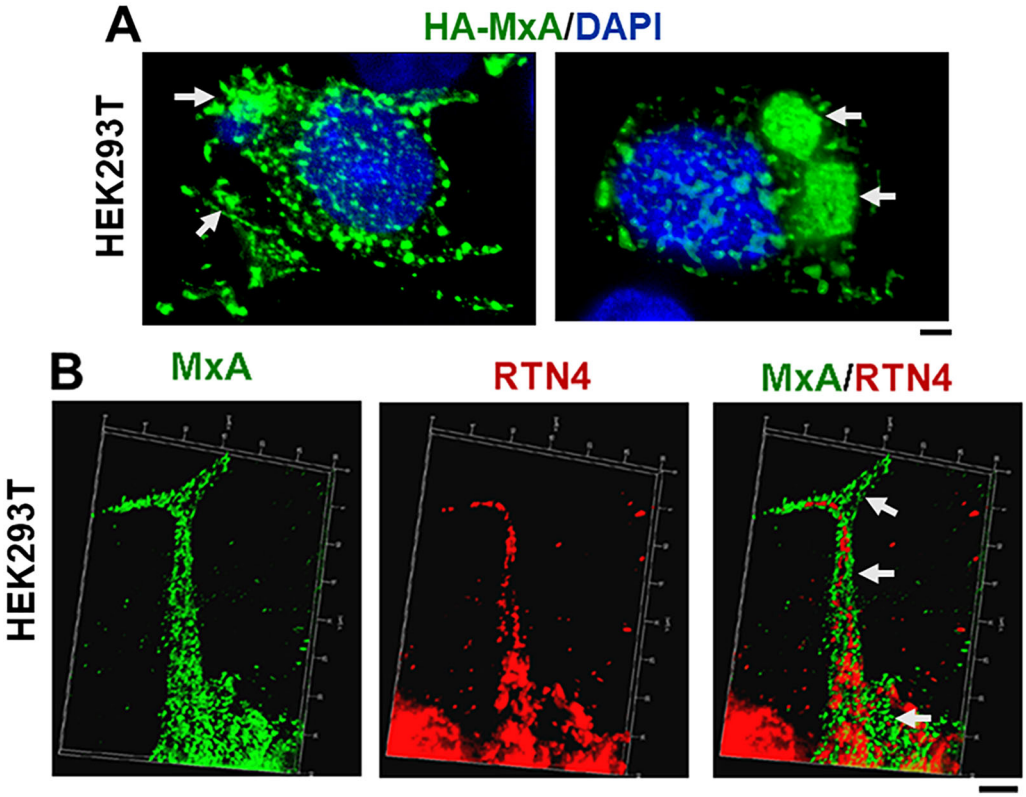

Figure 1. MxA forms variably sized and shaped mesoscale structures in the cytoplasm distinct from the endoplasmic reticulum (ER). Cultures of human HEK293T cells grown in 35 mm plates were transiently transfected the pHA-MxA expression vector (obtained from Stertz *et al.* 2006), fixed 1–2 days later, permeabilized using a digitonin-containing buffer, and the distribution of MxA and the ER structural protein reticulon-4 (RTN4) evaluated using immunofluorescence methods (imaged using an 100x oil immersion objective and z-stack data collection). Panel A, MxA structures in transiently transfected HEK293T cells (Scale bar = 10 μm). Arrows point to large compact mesoscale MxA-positive structures as observed in 25–35% of transfected cells. Panel B, MxA granular structures were distinct from the RTN4-positive ER. Scale bar = 5 μm. Adapted from Yuan and Sehgal (2016) and Davis *et al.* (2019).

present in Huh7 hepatoma cells (figure 3; Davis *et al.* 2018 2019 and Sehgal *et al.* 2020a, b), thus accounting for the observations of Stertz *et al.* 2006. Indeed, thin-section electron microscopy studies using CLEM methods confirmed the juxtaposition of membraneless MxA structures adjacent to but distinct from intermediate filaments (Davis *et al.* 2018 2019) consistent with the immunofluorescence images in figure 3. The further observation by us in June-July 2018 that exposure of Huh7 cells to hypotonic buffer led to the disassembly of GFP-MxA structures within 1–2 min, and that replenishment with isotonic culture medium led to rapid reassembly of the GFP-MxA structures (within 1 min) led us to an understanding of cytoplasmic MxA structures as metastable biomolecular membraneless condensates (figure 4; Davis *et al.* 2019). The GFP-MxA condensates could be cycled through at least three such rounds of hypotonic disassembly and isotonic reassembly (figure 4). These GFP-MxA structures were also rapidly disassembled by 1,6-hexanediol and had fluorescence recovery properties after photobleaching (FRAP) consistent with a gel-like consistency further confirming their identification as membraneless biomolecular condensates (Davis *et al.* 2019).

This paradigm shift has led us forward along two paths – the first to address questions about the condensate nature of human MxA structures in the cytoplasm and murine Mx1 structures in the nucleus (table 1), and the second to conduct extensive data mining of the Mx literature as part of the process of reinterpreting previous observations. As one example, we now infer that the membraneless human MxB structures juxtaposed to nuclear pores observed in 2004 by King *et al.* by electron microscopy also likely represent biomolecular condensates (table 1).

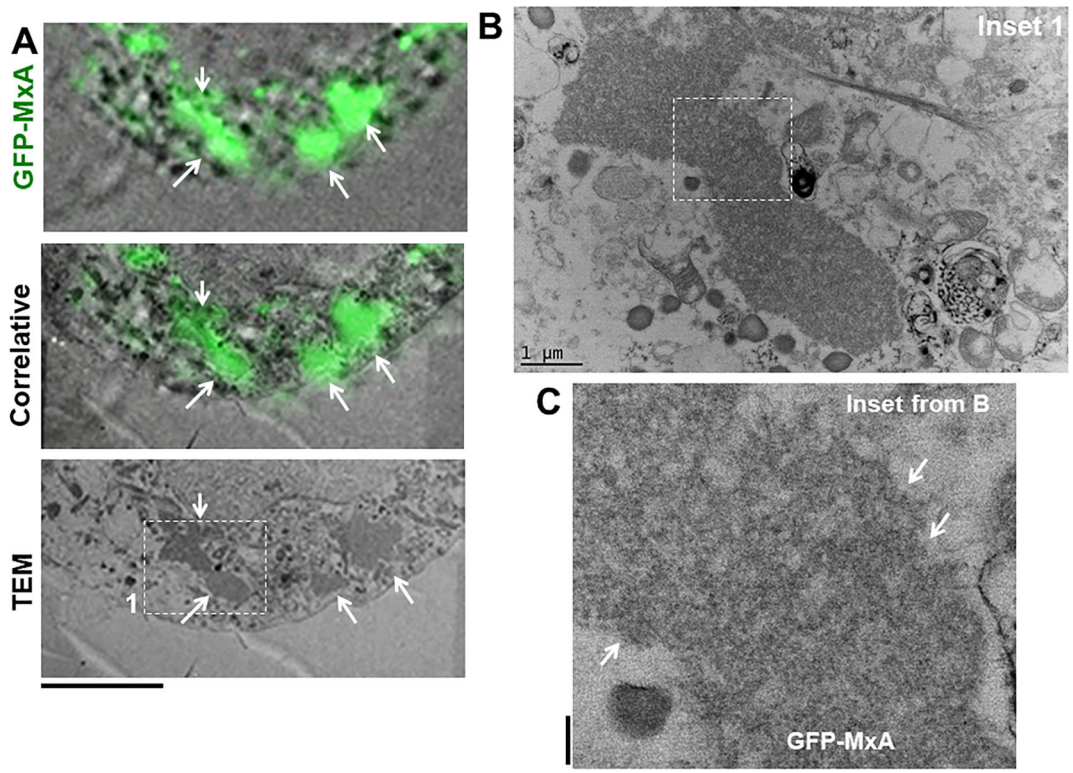

Figure 2. Correlated light and electron microscopy (CLEM) for identification of membraneless organelles. Huh7 cells plated sparsely in 35 mm gridded coverslip plates (MatTek) were transiently co-transfected with the pGFP-MxA vector. Two days later the cultures were fixed with 4% paraformaldehyde for 1 h at 4^0. Confocal imaging was carried out using a tiling protocol to identify the location of specific cells with GFP-MxA structures on the marked grid. The cultures were then further fixed, embedded and the previously identified grid locations used for serial thin-section EM (TEM). The tiled light microscopy data were correlated with the tiled EM data to identify the ultrastructure of the GFP-fluorescent structures (arrows in Panel A). Scale bar = 5 µm. Panel B shows a higher magnification image of inset 1 indicated in bottom image in Panel A. Scale bar = 1 µm. Panel C shows a higher magnification TEM images of the boxed portion in Panel B. Arrows indicate the absence of an enveloping membrane. Scale bar = 200 nm. Figure adapted from Davis *et al.* (2019).

Clearly at this time, there are many unanswered questions. The reader is referred to previous detailed reviews on the biology of Mx proteins in the context of innate immunity (Haller *et al.* 2015 2018). At this time, it would be premature for us tie aspects of the cell biology of Mx condensates (assembly/disassembly and metastability) to the broader biology of Mx proteins (antiviral activity against different viruses). Also, at this time, we are unaware of the identification of other dynamin-family large GTPases or other IFN-induced proteins that form biomolecular condensates (we are sure that these will come to be identified soon). The focus of this overview is to provide an interim summary of our data which helped identify cytoplasmic MxA and nuclear Mx1 structures as biomolecular condensates. It should be apparent from this Introduction that we are the only research group in the Mx field that has moved in this direction at this time.

3. Ubiquity of biomolecular condensates and phase-separated membraneless organelles (MLOs)

As a general comment, in addition to various membrane-bound subcellular compartments, the eukaryotic cell contains organized membraneless biomolecular condensates of proteins and nucleic acids which form functional organelles (Mitrea and Kriwacki 2016; Banani *et al.* 2017; Shin and Brangwynne 2017; Alberti 2017; Gomes and Shorter 2019; Alberti *et al.* 2019; Sehgal *et al.* 2020a). Examples include the nucleolus, the nucleoporin granules, nuclear speckles and paraspeckles, nuclear promyelocytic leukemia (PML) bodies, nuclear Cajal bodies, cytoplasmic processing (P) bodies, germinal P bodies, Balbiani bodies, Negri bodies, stress granules, translation promoting TPA-inducible sequence 11b (TIS) granules, cytoplasmic and nuclear viral replication and maturation

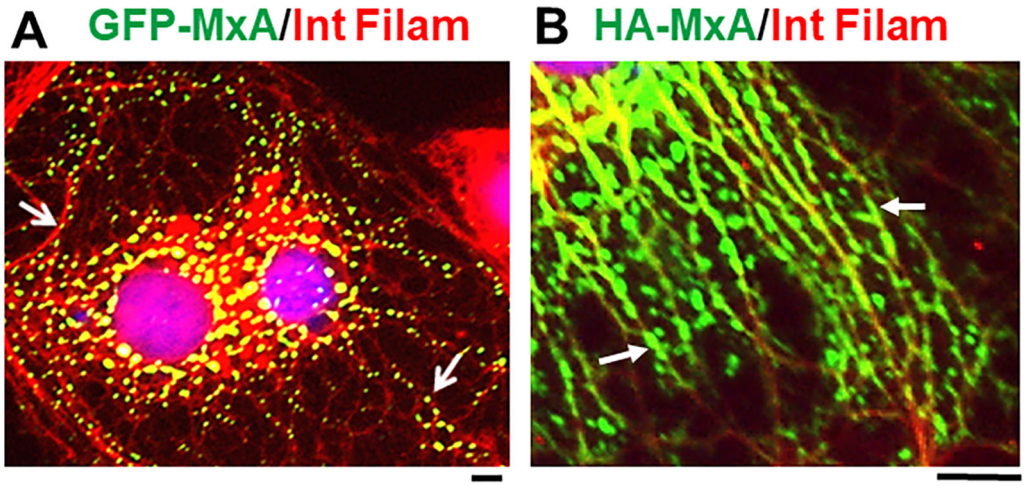

Figure 3. HuMxA condensates in Huh7 hepatoma cells often use intermediate filaments as scaffolding. Human hepatoma Huh7 cells cultured in 35 mm plates were transiently transfected with expression vector for GFP-MxA (Panel **A**) or HA-MxA (Panel **B**). Two days later the cultures were fixed and imaged for GFP-MxA (Panel **A**, by fluorescence in green), HA-MxA (Panel **B**, by immunofluorescence using anti-HA mAb in green), and intermediate filaments (Panels **A** and **B**, using anti-giantin pAb in red; see Sehgal *et al.* 2020b for validation). White arrows point to spherical GFP-MxA structures and streaks of HA-MxA adhering to intermediate filaments in Panels **A** and **B** respectively. Scale bars = 5 μm. Adapted from Davis *et al.* (2019) and Sehgal *et al.* (2020a).

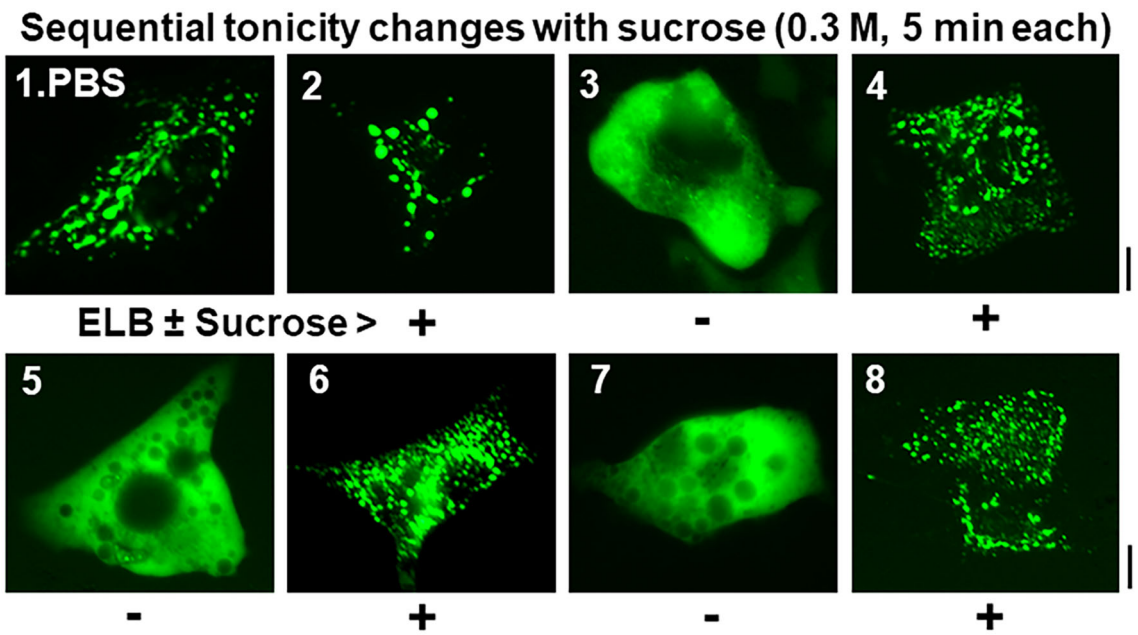

Figure 4. Repetitive tonicity-driven disassembly and reassembly of GFP-MxA condensates. A culture of Huh7 cells in 35 mm plate transiently expressing GFP-MxA kept continuously at 37 °C was sequentially imaged in 5 min steps in the indicated media [warm isotonic phosphate buffered saline (PBS) or warm hypotonic erythrocyte lysis buffer (ELB) without or with supplementation with 0.3M sucrose indicated (− or +)]. Images 1–8 illustrate representative examples of cells at each stage in the same culture (out of 10–20 images per step). Scale bars = 10 μm. Figure adapted from Davis *et al.* (2019).

complexes, and several more recent discoveries such as condensates of synapsin, of the DNA sensor protein cyclic GMP-AMP synthase (cGAS) in the cytoplasm, the cytoplasmic antiviral proteins human MxA, the nuclear antiviral protein murine Mx1, and active transcription- and splicing-associated condensates in the nucleus. Overall, these condensates have liquid-like internal properties and alter shape and consistency (are 'metastable') changing from liquid-like to a gel and/or to filaments and even undergo disassembly/reassembly

cycles commensurate with the cellular environment (temperature, ionic conditions and tonicity, physical deformation or cytoplasmic 'crowding'), and the incorporation of additional proteins, RNA or DNA molecules or posttranslational modifications (Mitrea and Kriwacki 2016; Banani *et al.* 2017; Shin and Brangwynne 2017; Alberti 2017; Alberti *et al.* 2019; Gomes and Shorter 2019; Sehgal 2019; Davis *et al.* 2018 2019; Sehgal *et al.* 2020a, b; Du and Chen 2018; Milovanovic *et al.* 2018; Delarue *et al.* 2018; Boke *et al.* 2016; Sabari *et al.* 2018; Ditlev *et al.* 2018; Rai *et al.* 2018; Boeynaems *et al.* 2019; Ma and Mayr 2018). Indeed, DNA and RNA molecules specifically participate in the assembly of such cytoplasmic and nuclear condensates and in their function (Mitrea and Kriwacki 2016; Banani *et al.* 2017; Shin and Brangwynne 2017; Alberti 2017; Alberti *et al.* 2019; Gomes and Shorter 2019; Du and Chen 2018; Milovanovic *et al.* 2018; Delarue *et al.* 2018; Boke *et al.* 2016; Sabari *et al.* 2018; Ditlev *et al.* 2018; Ma and Mayr 2018). Moreover, in many instances the dynamic assembly, disassembly and reassembly of such condensates within a cell compartment is regulated during differentiation, cell cycle, stress and under pathological conditions (reviewed in Rai *et al.* 2018; Gomes and Shorter 2019; Sehgal 2019; Sehgal *et al.* 2020a). Collectively, such condensates form a hierarchy of distinct membraneless organelles (MLOs) in the cytoplasm and nucleus which serve distinct cellular functions.

4. Different Mx GTPase protein family members form biomolecular condensates in different subcellular compartments

The Mx proteins are now established as the major antiviral effectors of Type I (IFN-α/β) and Type III (IFN-λ), but not Type II (IFN-γ) interferons (Kochs *et al.* 2002; Haller and Kochs 2002; Haller *et al.* 2007 2015; Verhelst *et al.* 2013) (figure 5). The Mx proteins are now recognized to inhibit a broad spectrum of RNA- and DNA-containing viruses (Haller and Kochs 2002; Haller *et al.* 2015 2018; Verhelst *et al.* 2013). Mx proteins are large dynamin-family GTPases of size 60–70 kDa which readily multimerize into rings and filaments and contain intrinsically disordered regions (e.g. the L4 loop) which contribute to multimerization (figure 5) (Haller *et al.* 2015). There are two human Mx proteins (MxA and MxB) and two murine Mx proteins (Mx1 and Mx2) of different antiviral activities and different subcellular localizations – cytoplasmic vs. nuclear (table 1, figure 5). To clarify the nomenclature of the Mx protein family we adopt the gene lineage tracing presented by Busnadiego *et al.* (2014) and Haller *et al.* (2015) as follows: most mammalian Mx proteins are formed from two distinct gene lineages (*MxA* or *MxB*) that arose from an ancient duplication event. Thus, humans have two Mx proteins – MxA and MxB (some investigators call these as human Mx1 and human Mx2 respectively although the terms Mx1 and Mx2 are correctly reserved for murine Mx proteins). Although mice also have two Mx genes – *Mx1* and *Mx2*, both these are paralogous members of the human *MxA* lineage. Thus, human *MxB* (which is also called human *Mx2* by some investigators) and murine *Mx2* are *not* orthologous. We use the terms MxA or HuMxA for the human protein, and Mx1 or MuMx1 for the orthologous murine protein. Parenthetically, rats have three Mx proteins Mx1, Mx2 and Mx3 (Haller *et al.* 2015). Rat Mx1 and rat Mx2 are orthologs of human MxA, have antiviral activity and form nuclear and cytoplasmic granules respectively, while rat Mx3 is diffuse in the cytoplasm and lacks antiviral activity.

Human MxA forms cytoplasmic structures while murine Mx1 mainly forms nuclear bodies (table 1; figure 6; Haller and Kochs 2002; Kochs *et al.* 2002; Engelhardt *et al.* 2004; Haller *et al.* 2015; Sehgal *et al.* 2020b). The molecular mechanisms of the Mx antiviral effects are incompletely understood; these effects include inhibition of early and late viral transcription and viral replication, as well as effects at the level of the transit of viral components through the nuclear pore (Haller and Kochs 2002; Verhelst *et al.* 2013; Haller *et al.* 2015; Steiner and Pavlovic 2020). It is only in the last 3 years that we recognized that human MxA formed metastable membraneless biomolecular condensates in the intact-cell cytoplasm, and only in the last year that murine Mx1 formed biomolecular condensates mainly in the nucleus, but also in the cytoplasm in some cells (figure 6; reviewed in Sehgal *et al.* 2020a, b). Both the cytoplasmic HuMxA bodies and nuclear MuMx1 bodies comprised phase-separated membraneless organelles (MLOs) with a gel-like internal consistency (as tested using fluorescence recovery after photobleaching (FRAP) methods) (Davis *et al.* 2019; Sehgal *et al.* 2020a, b). Additionally, HuMxB forms cytoplasmic membraneless structures juxtaposed to the cytoplasmic side of nuclear pores (Table 1) (King *et al.* 2004; Goujon *et al.* 2013; reviewed in Sehgal *et al.* 2020b; Steiner and Pavlovic 2020).

Remarkably, it is also now recognized that replication/maturation of many viruses also involves phase-separated liquid droplets [e.g. vesicular stomatitis (VSV), rabies (Negri bodies), influenza A, Ebola, measles, Epstein-Barr, and even SARS-CoV-2 viruses] (reviewed

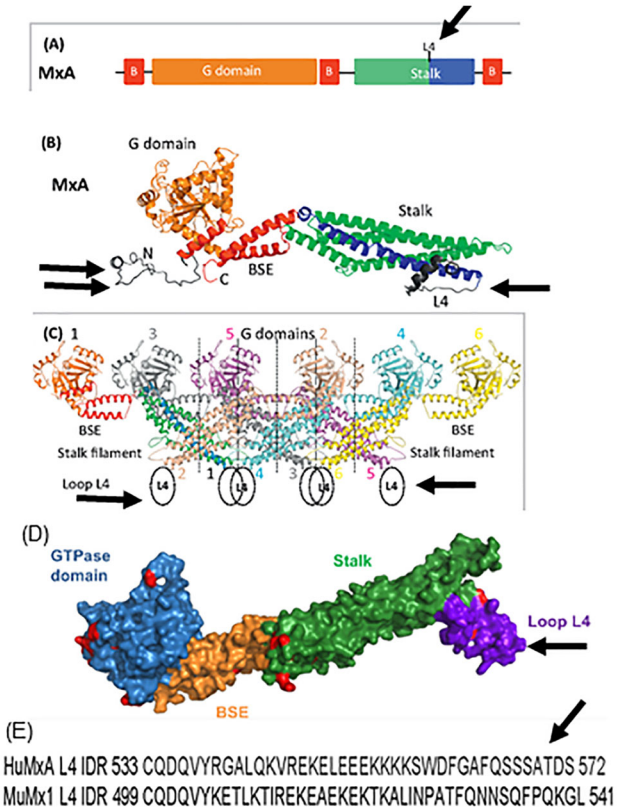

Figure 5. Key features of the structure of MxA monomers and oligomers. Panels **A** and **B**, schematic and 3D structure of respective color-coded domains in MxA GTPase monomers. The GTPase G domain forms the head group, the Stalk consists of three α helices which help drive oligomerization, while the BSE hinge region is made up of α-helices from three different portions of the MxA sequence (labelled 'B' in Panel **A**. L4 (single arrow) represents the polylysine intrinsically disordered domain (IDR), while the double arrow points to a disordered domain at the N terminus. Panel **C**, Structure of MxA oligomers (linear or ring shaped) formed in cell-free assays driven by the stalk filaments and by the L4 loops (arrow). Panel **D**, Space-filling model of the MxA monomer highlighting the exposed location of the L4 IDR region (arrow). Panel **E**, Comparison of the sequences of the IDR loop L4 in HuMxA and MuMx1. Modified from Haller *et al.* (2015) with permission.

in Sehgal *et al.* 2020a, b). It is noteworthy that MxA cytoplasmic condensates in virus infected cells incorporate respective viral nucleocapsid proteins (table 1) (Kochs *et al.* 2002; Davis *et al.* 2019; reviewed in Sehgal *et al.* 2020a, b). Overall, human MxA forms disparate membraneless structures solely in the cytoplasm and has antiviral activity towards several RNA- and DNA-containing viruses including orthomyxo- and rhabdoviruses (Haller *et al.* 2015; Sehgal *et al.* 2020a, b). Human MxB is mainly associated with the cytoplasmic side of nuclear pores (through an N-terminal nuclear localization signal, NLS) and additional cytoplasmic membraneless structures. Full-length MxB has antiviral activity against HIV and other lentiviruses, and herpesviruses by blocking entry of viral components into the nucleus, but not against influenza A virus (FLUAV) (King *et al.* 2004; Goujon *et al.* 2013; reviewed in Haller *et al.* 2015 and in Steiner and Pavlovic 2020). However, ectopic expression of genetically modified MxB targeting it to the cytoplasm (using the N-terminal 43 amino acid segment from MxA) or nucleus (using the T-antigen NLS) renders MxB antiviral towards FLUAV (Steiner and Pavlovic 2020).

Murine Mx1 is mainly in nuclear bodies (it has a 'weak' C-terminal NLS, Zürcher *et al.* 1992a, b, c), while murine Mx2 is mainly in cytoplasmic structures (Zürcher *et al.* 1992c; Haller *et al.* 2015). In terms of antiviral activity, the nuclear murine Mx1 has antiviral activity towards influenza virus (FLUAV) (which has an obligate nuclear transcription step) but not vesicular stomatitis virus (VSV) (replicates entirely in the cytoplasm), while the cytoplasmic granular murine Mx2 has antiviral activity towards VSV but not FLUAV (Haller *et al.* 2015; table 1). Curiously, the nuclear-predominant rat Mx1 has antiviral activity towards both FLUAV and VSV, while the cytoplasmic-predominant rat Mx2 is antiviral towards VSV only (Verhelst *et al.* 2013; Haller *et al.* 2015). Rat Mx3, which is mainly dispersed in the cytoplasm, has little apparent antiviral activity (Verhelst *et al.* 2013; Haller *et al.* 2015). Although murine Mx1 artificially deleted of its C-terminal NLS is cytoplasmic it remains inactive against VSV (Zürcher *et al.* 1992a, 1992b). In contrast, wild-type GFP-MuMx1 expressed in human hepatoma Huh7 cells associates with cytoplasmic intermediate filaments and now shows antiviral activity against VSV (Sehgal *et al.* 2020b, table 1 and figures 7 and 8 below). Thus, the different subcellular localizations of MLOs of different Mx proteins contribute to their respective antiviral activities. Our overall focus is to understand the formation, dynamics and function of different antiviral Mx biomolecular condensates. The objective is to move the field of antiviral Mx proteins into the realm of phase-separated membraneless organelles (MLOs) and biomolecular condensates, and set the stage for detailed proteomics studies in the future of the composition of Mx condensates.

5. Metastability of biomolecular condensates of Mx proteins

Cytoplasmic human MxA condensates and nuclear murine Mx1 condensates (figure 6) comprised dramatically metastable (shape-changing) phase-separated

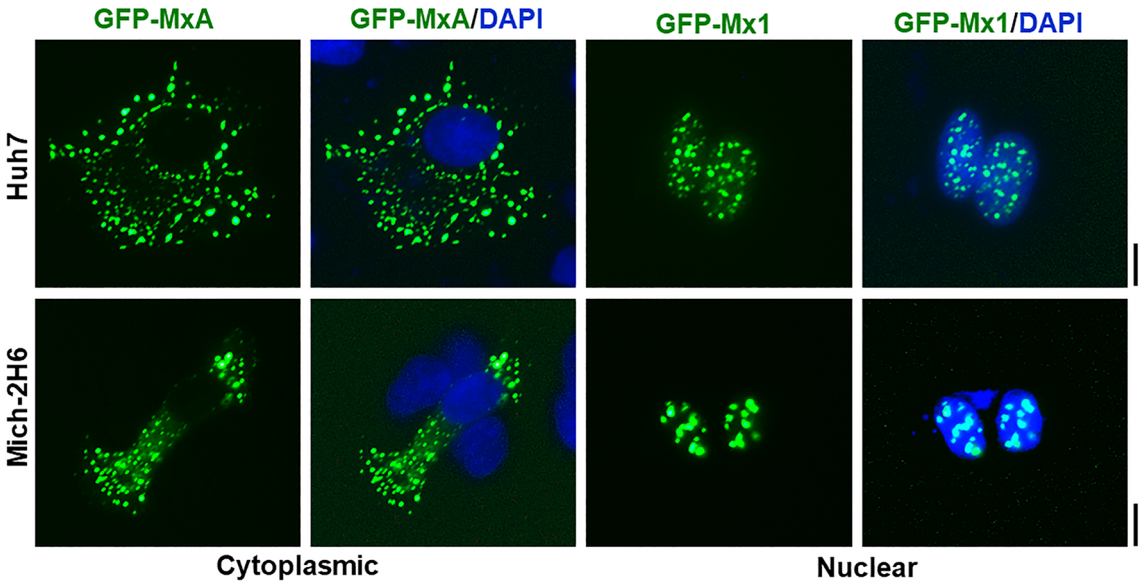

Figure 6. Comparison of subcellular localization of human GFP-MxA with murine GFP-Mx1 in two different cell lines. Cultures of Huh7 hepatoma and Mich-2H6 melanoma cells in 35 mm plates were transiently transfected with expression vectors for human GFP-MxA or murine GFP-Mx1, fixed using 4% paraformaldehyde 2 days later, additionally stained with DAPI to visualize the nuclei, and imaged using two-color fluorescence. The figure illustrates representative cells. None of the cells transfected with human GFP-MxA vector showed any MxA in nuclei; 70–80% of Huh7 cells transfected with GFP-Mx1 showed only nuclear Mx1 (for cells with cytoplasmic GFP-Mx1 structures see figures 7 and 8); almost all of Mich-2H6 cells transfected with GFP-Mx1 showed only nuclear GFP-Mx1 bodies. Scale bars = 10 μm. From Sehgal *et al.* (2020b).

MLOs (Davis *et al.* 2018 2019; Sehgal *et al.* 2020a, b; table 1). These GFP-MxA and GFP-Mx1 condensates were disassembled by 1,6-hexanediol (and were thus liquid-like phase separated structures) (Davis *et al.* 2019). Disassembly of nuclear GFP-Mx1 bodies by hexanediol was than that of cytoplasmic GFP-MxA bodies (Sehgal *et al.* 2020b). Both cytoplasmic GFP-MxA and nuclear GFP-Mx1 condensates showed a gel-like internal consistency in FRAP assays with approximately 18–20% internal mobility) (Davis *et al.* 2019; Sehgal *et al.* 2020b). Importantly, IFN-α-induced endogenous MxA in human cells also formed cytoplasmic condensates (Davis *et al.* 2018 2019; Sehgal *et al.* 2020a).

As another aspect of their metastability, both cytoplasmic GFP-MxA condensates and nuclear GFP-Mx1 condensates were disassembled by exposing cells to hypotonic buffer (ELB), and then reassembled upon shifting cells to isotonic buffer (figure 4; Davis *et al.* 2019; Sehgal *et al.* 2020b). This hypotonicity-driven disassembly/metastability is reminiscent of conditions of cells with intracellular edema. This metastability was also observed for GFP-Mx1 nuclear condensates in homologous murine cells (NIH 3T3) (Sehgal *et al.* 2020b). We interpret hypotonic disassembly/isotonic reassembly as resulting from rapid cytoplasmic uncrowding and recrowding mechanisms (i.e. responsive to cytoplasmic swelling and its reversal) (Davis *et al.* 2019; Sehgal *et al.* 2020a, b).

Live-cell imaging confirmed that spherical cytoplasmic MxA condensates underwent homotypic fusion (Davis *et al.* 2019). There was further metastability in terms of a spherical to filamentous change when cells were exposed to physical compression and/or hypoxia (by placement on a coverslip on live cells), nitric oxide scavenging (by c-PTIO) or inhibition of GTPase activity (by dynasore) (Davis *et al.* 2019). The unanswered question at the moment is whether these changes influence antiviral activity.

6. Heterogeneity of condensates of Mx proteins

As with stress granules (Ditlev *et al.* 2018; Shiina 2019), there is structural heterogeneity in cytoplasmic MxA condensates, especially the presence of a detergent (saponin) resistant core in some condensates (Davis *et al.* 2019). MxA condensates disassembled upon saponin permeabilization of the plasma membrane of cells consistent with an 'uncrowding' mechanism regulating MxA condensate structure. Additionally, 20–30% of cells retained saponin-

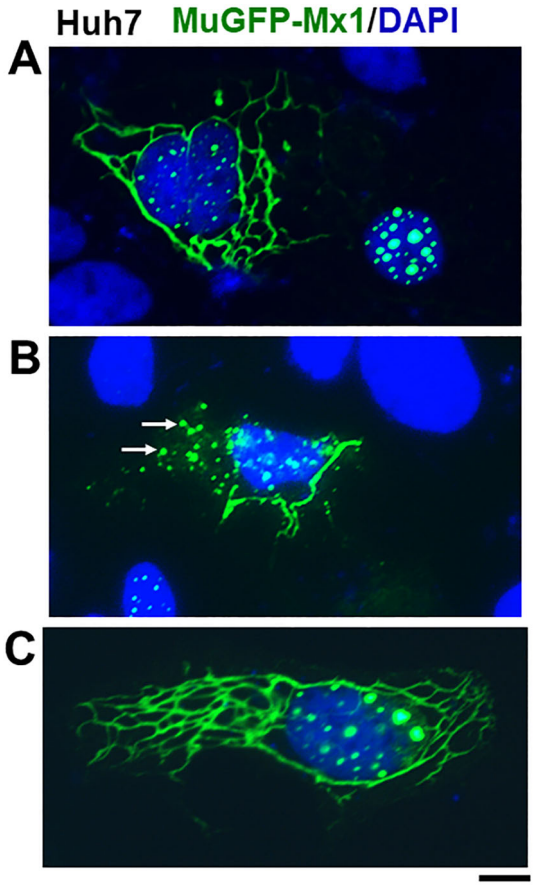

Figure 7. Spherical nuclear, spherical cytoplasmic and filamentous cytoplasmic condensates of murine GFP-Mx1. Cultures of Huh7 cells in 35 mm plates were transiently transfected with the expression vector for murine GFP-Mx1. Two days later the cultures were fixed using 4% paraformaldehyde, permeabilized using the 0.05% Triton buffer, and stained with DAPI to visualize the nuclei, and imaged using two-color fluorescence. Approximately 20–30% of transfected cells showed cytoplasmic murine GFP-Mx1 as shown in Panels A, B and C. Panel A shows two adjacent cells – one showing GFP-Mx1 exclusively in nuclear bodies and one cell with GFP-Mx1 present extensively in cytoplasmic filaments and cytoplasmic structures. Panel B shows adjacent cells – one with extensive cytoplasmic filaments and cytoplasmic bodies (arrows) of GFP-Mx1 and the other showing a nucleus with only nuclear GFP-Mx1 bodies (at lower edge). Panel C shows a cell with both nuclear GFP-Mx1 bodies and cytoplasmic filaments. Modified from Sehgal *et al.* (2020b).

resistant 'cores' of GFP-MxA condensates (Davis *et al.* 2019). Thus, in future studies, we shall follow the paradigm established in studies of stress granule components (Banani *et al.* 2017; Ditlev *et al.* 2018; Alberti *et al.* 2019; Shiina 2019), by first identifying components of MxA condensate cores, before exploring the more transient association of other client proteins with these structures.

While human GFP-MxA structures were exclusively cytoplasmic, and murine GFP-Mx1 structures mainly nuclear (as in figure 6), a subset of cells (in human Huh7 and murine NIH3T3 cell lines) transiently expressing MuGFP-Mx1 showed accumulation of this protein in cytoplasmic bodies and filaments (figure 7) (Sehgal *et al.* 2020b). This formation of cytoplasmic GFP-Mx1 structures was not a consequence of overexpression of the recombinant protein but occurred even when there was only low level of expression of GFP-Mx1 (Sehgal *et al.* 2020b). In Huh7 cells, these cytoplasmic filaments of GFP-Mx1 consisted of vimentin-positive intermediate filaments (Sehgal *et al.* 2020b). The possibility that, in contrast to GFP-HuMxA structures which lie adjacent to intermediate filaments (figure 3A), the GFP-MuMx1 might be part of the structure of intermediate filaments remains open.

This heterogeneity of subcellular location of MuGFP-Mx1 condensates was reflected in differences in antiviral properties (Sehgal *et al.* 2020b). Using single-cell-based assays for antiviral activity towards VSV, on the one hand we were able to confirm that cytoplasmic human MxA was antiviral towards VSV, but that nuclear murine Mx1 was not (figure 8). On the other hand, cells exhibiting cytoplasmic filamentous wild-type MuGFP-Mx1 had an antiviral effect against VSV (figure 8). These data emphasize the occurrence of a broader antiviral spectrum of Mx proteins in different cell types based upon the subcellular cytoplasmic compartment in which the respective Mx proteins form condensates (Haller *et al.* 2015; Sehgal *et al.* 2020b; also see Steiner and Pavlovic 2020 for MxB).

7. Comments

Overall, our new data show that (a) both human MxA and murine Mx1 give rise to metastable phase-separated biomolecular condensates, albeit in different subcellular compartments (cytoplasm vs. nucleus respectively), (b) when in the cytoplasm, both human MxA and murine Mx1 can associate with intermediate filaments, and (c) both human MxA and murine Mx1 when cytoplasmic exhibit an antiviral activity towards VSV – a rhabdovirus which replicates and matures entirely in the cytoplasm (table 1). The data showing the close relationship between membraneless MxB structures and nucleoporins on the cytoplasmic face of nuclear pores and the involvement of MxB in regulating cargo transit through the pore channel (King

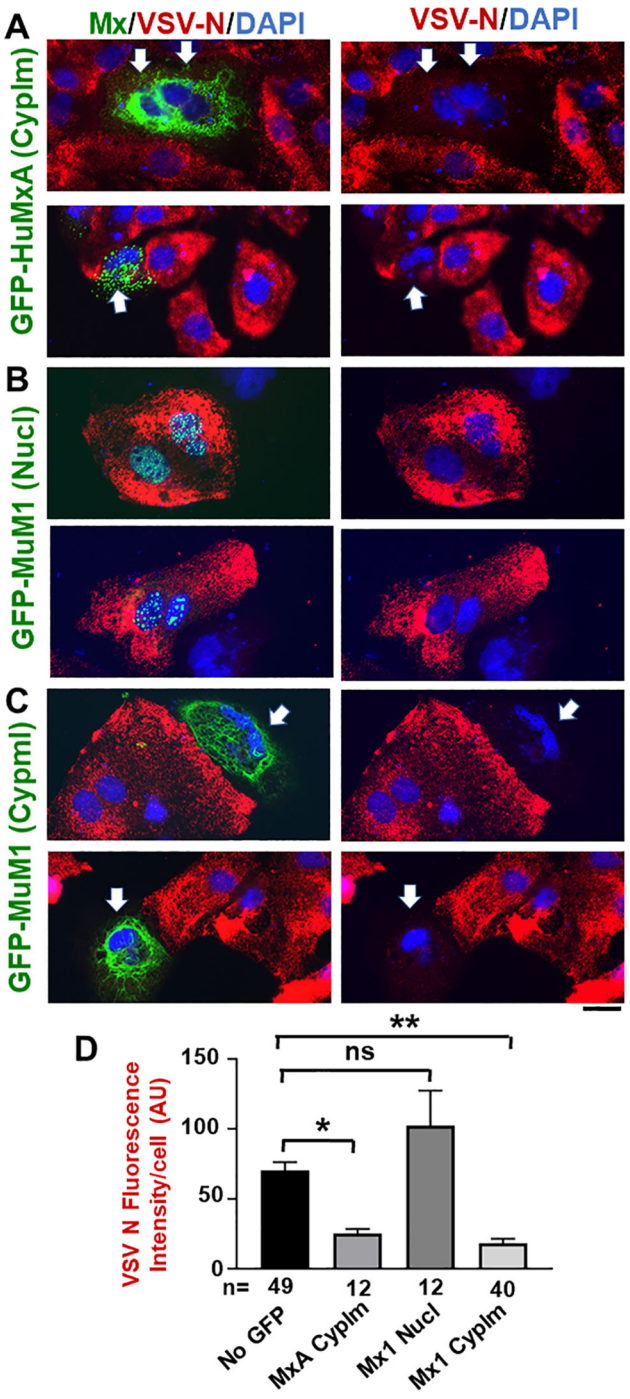

◄**Figure 8.** Differences in subcellular localization of MuGFP-Mx1 condesnates (in cytoplasm vs. nucleus) affects antiviral activity towards VSV. Huh7 cells (approx. 2×10^5) per 35 mm plate, transfected with the GFP-HuMxA (as a positive control) or GFP-MuMx1 expression vectors 2 days earlier, were replenished with 0.25 ml serum-free Eagle's medium and then 20 µl of a concentrated VSV stock of the wt Orsay strain added (corresponding to multiplicity of infection >10 plaque forming units/cell). The plates were rocked every 15 min for 1 hr followed by addition of 1 ml of full culture medium. The cultures were fixed with 4% paraformaldehyde at 4 hr after the start of the VSV infection and the extent of VSV N protein expression in individual cells evaluated using immunofluorescence methods (using the mouse anti-N mAb) and Image J for quantitation. Panels **A**, **B** and **C** illustrate representative cells showing the absence of any GFP, or the appearance of cytoplasmic GFP-HuMxA, nuclear GFP-MuMx1 or cytoplasmic GFP-MuMx1 and the corresponding level of expression of viral N protein (thick arrows point to cells displaying an antiviral effect). All scale bars = 20 µm. Panel **D**, enumerates N protein expression in various classes of cells shown in Panels **A**, **B** and **C** imaged at identical exposure settings and expressed in arbitrary fluorescence units (AU) per cell. n= number of cells evaluated per group in this experiment (for this evaluation cells with only cytoplasmic Mx1 were combined with cells with both cytoplasmic and nuclear Mx1); vertical columns depict Mean ±SE. Statistical significance was evaluated using ANOVA (Kruskal-Wallis with Dunn's post-test for multiple comparisons); * $P < 0.01$; ** $P < 0.001$; ns, not significant ($P > 0.05$). Adapted from Sehgal *et al.* (2020b).

et al. 2004; Goujon *et al.* 2013; reviewed in Steiner and Pavlovic 2020) allow us to now suggest that MxB structures at and near nuclear pores also represent phase-separated biomolecular condensates (table 1; Sehgal *et al.* 2020b).

Murine Mx1 typically shows antiviral activity towards influenza A virus (FLUAV) and other orthomyxoviruses which require a nuclear step in their replication, but not towards rhabdoviruses such as VSV which replicate entirely in the cytoplasm (Verhelst *et al.* 2013; Haller *et al.* 2015) (table 1). In contrast, functional murine Mx2 (isolated from feral mice) was observed to display an antiviral activity towards VSV but not FLUAV (Verhelst *et al.* 2013; Haller *et al.* 2015). Commensurately, while murine Mx1 was observed to be in nuclear bodies, murine Mx2 was observed to be mainly in granular cytoplasmic structures (Haller *et al.* 2015), which might perhaps also represent biomolecular condensates (table 1). Moreover, we observed that a subset of cells expressing murine GFP-Mx1 express this protein in cytoplasmic bodies and filaments. Using single-cell-based assays for VSV replication we discovered that cells that expressed cytoplasmic wild-type GFP-Mx1, but not those exhibiting only nuclear GFP-Mx1 condensates, displayed an antiviral effect against this virus – a virus which replicates solely in the cytoplasm.

Mutational studies of human MxA show that the GTPase activity is required for most of its antiviral

activity (except that against hepatitis B virus) (Haller *et al.* 2015; Dick *et al.* 2015; Nigg and Pavlovic 2015; Steiner and Pavlovic 2020). Data in the literature also reveal that MxA mutants lacking GTPase activity can still form cytoplasmic condensates (Dick *et al.* 2015; Nigg and Pavlovic 2015). Mutations that cause dispersal of MxA in the cytoplasm (e.g. the D250N mutant) lacked antiviral activity (Dick *et al.* 2015; Steiner and Pavlovic 2020). The R645 point mutant of MxA, which was in larger cytoplasmic granules, had the unusual property of inhibiting FLUAV but not VSV, even though the wt MxA showed antiviral activity towards both viruses (Zürcher *et al.* 1992b). A mutational analysis of rat Mx2 showed that mutants that formed 'granular' cytoplasmic structures exhibited antiviral activity towards VSV, while those that were 'diffuse' in the cytoplasm did not (Zürcher *et al.* 1992c). These data suggest that condensate formation may be important but not sufficient for the antiviral activity of Mx proteins.

The hypotonicity-driven disassembly of Mx protein condensates in live cells (figure 4; Davis *et al.* 2019; Sehgal *et al.* 2020b) highlight an unusual aspect of Mx protein chemistry. The biochemical basis for this hypotonicity driven disassembly may reflect the effect of cytoplasmic 'crowding' on higher-order protein structure or rapid changes due to hypotonicity-triggered post-translational modifications.

At this time there are many unanswered questions related to the biochemical mechanisms involved in the formation and metastability of Mx condensates in the cell cytoplasm and the nucleus. The structural contributions of intrinsically disordered domains (IDRs) in Mx proteins (the L4 loop and the N-terminal region; figure 5) to condensate formation remain to be investigated. The relationship between condensate formation and antiviral activities remains unclear. Nevertheless, it is already clear that subcellular localization of Mx condensates is an important determinant of antiviral specificity. The key paradigm shift in the last three years has been to move the Mx field away from the widely prevalent interpretation that MxA associates with intracellular membranes (e.g. the endoplasmic reticulum) towards consideration of Mx structures as membraneless organelles (MLOs).

Acknowledgements

This work was supported by a grant from the New York Medical College, and by personal funds of PBS.

References

Accola MA, Huang B, Masri AA and McNevin MA 2002 The antiviral dynamin family member, MxA, tubulates lipids and localizes to the smooth endoplasmic reticulum. *J. Biol. Chem.* **277** 21829–21835

Alberti S 2017 The wisdom of crowds: regulating cell function through condensed states of living matter. *J Cell Sci.* **130** 2789–2796

Alberti S, Gladfelter A and Mittag T 2019 Considerations and challenges in studying liquid-liquid phase separation and biomolecular condensates. *Cell* **176** 419–434

Banani SF, Lee HO, Hyman AA and Rosen MK 2017 Biomolecular condensates: organizers of cellular biochemistry. *Nat. Rev. Mol. Cell Biol.* **18** 285–298

Boeynaems S, Holehouse AS, Weinhardt V, Kovacs D, Lindt JV, *et al*. 2019 Spontaneous driving forces give rise to protein-RNA condensates with coexisting phases and complex material properties. *Proc. Natl. Acad. Sci. USA* **116** 7889–7898

Boke E, Ruer M, Wuhr M, Coughlin M, Lemaitre R, *et al*. 2016 Amyloid-like self-assembly of a cellular compartment. *Cell* **166** 637–650

Busnadiego I, Kane M, Rihn S, Preugchau HF, Hughes J, *et al*. 2014 Host and viral determinants of Mx2 antiretroviral activity. *J. Virol.* **88** 7738–7752

Davis D, Yuan H, Yang YM, Liang FX and Sehgal PB 2018 Interferon-alpha- induced cytoplasmic MxA structures in hepatoma Huh7 and primary endothelial cells. *Contemp Oncol (pozn)* **22** 86–94

Davis D, Yuan H, Liang FX, Yang YM, Westley J, *et al*. 2019 Human antiviral protein MxA forms novel metastable membraneless cytoplasmic condensates exhibiting rapid reversible tonicity- driven phase transitions. *J. Virol.* **93** e01014–e01019

Delarue M, Brittingham GP, Pfeffer S, Surovtsev IV, Pinglay S, *et al*. 2018 mTORC1 Controls phase separation and the biophysical properties of the cytoplasm by tuning crowding. *Cell* **174** 338–349

Desai SM 1970 Sarcoma blockade *in vivo:* rabies-Rous system in chickens. *Nature* **228** 460–461

Desai SM, Sehgal PB, Nanavati AND and Shirodkar MV 1973 A rabies-induced serum factor inhibiting Rous sarcoma virus in chickens. *J. Gen. Virol.* **19** 285–293

Dick A, Graf L, Olal D, von der Malsburg A, Gao S, *et al*. 2015 Role of nucleotide binding and GTPase domain dimerization in dynamin-like myxovirus resistance protein A for GTPase activation and antiviral activity. *J. Biol. Chem.* **290** 12779–12792

Ditlev JA, Case LB and Rosen MK 2018 Who's in and who's out - compositional control of biomolecular condensates. *J. Mol. Biol.* **430** 4666–4684

Du M and Chen ZJ 2018 DNA-induced liquid phase condensation of cGAS activates innate immune signaling. *Science* **361** 704–709

Engelhardt OG, Sirma H, Pandolfi PP and Haller O 2004 Mx1 GTPase accumulates in distinct nuclear domains and inhibits influenza A virus in cells that lack promyelocytic leukemia protein nuclear bodies. *J. Gen. Virol.* **85** 2315–2326

Gomes E and Shorter J 2019 The molecular language of membraneless organelles. *J. Biol. Chem.* **294** 7115–7127

Goujon C, Moncorge O, Bauby H, Doyle T, Ward CC, *et al*. 2013 Human Mx2 is an interferon-induced post-entry inhibitor of HIV-1 infection. *Nature* **502** 559–562

Haller O and Kochs G 2002 Interferon-induced Mx proteins: dynamin-like GTPases with antiviral activity. *Traffic* **3** 710–717

Haller O, Arnheiter H, Gresser I and Lindenmann J 1979 Genetically determined, interferon-dependent resistance to influenza virus in mice. *J. Exp. Med.* **149** 601–612

Haller O, Staeheli P and Kochs G 2007 Interferon-induced Mx proteins in antiviral host defense. *Biochimie* **89** 812–818

Haller O, Staeheli P, Schwemmle M and Kochs G 2015 Mx GTPases: dynamin- like antiviral machines of innate immunity. *Trends Microbiol.* **23** 154–163

Haller O, Arnheiter H, Pavloviv J and Staehli P 2018 The discovery of the antiviral resistance gene Mx: a story of great ideas, great failures, and some success. *Annu Rev. Virol.* **5** 33–51

Henle W 1950 Interference phenomena between animal viruses: a review. *J. Immunol.* **64** 203–236

Ho M 1962 Interferons. *New Engl. J. Med.* **266** 1313–1318

Isaacs A and Lindenmann J 1957 Virus interference. I. The interferon. *Proc. R. Soc. Lond. B* **147** 258–267

Isaacs A, Lindenmann J and Valentine RC 1957 Virus interference. II. Some properties of interferon. *Proc. R. Soc. Lond. B* **147** 268–273

King MC, Raposo G and Lemmon MA 2004 Inhibition of nuclear import and cell-cycle progression by mutated forms of the dynamin-like GTPase MxB. *Proc. Natl. Acad. Sci. USA* **101** 8957–8962

Kochs G, Janzen C, Hohenberg H and Haller O 2002 Antivirally active MxA protein sequesters La Crosse virus nucleocapsid protein into perinuclear complexes. *Proc. Natl. Acad. Sci. USA* **99** 3153–3158

Lindenmann J 1962 Resistance of mice to mouse-adapted influenza A virus. *Virology* **16** 203–204

Lindenmann J 1964 Inheritance of resistance to influenza virus in mice. *Proc. Soc. Exp. Biol. Med.* **116** 506–509

Lindenmann J, Lane CA and Hobson D 1963 The resistance of A2G mice to myxoviruses. *J. Immunol.* **90** 942–951

Ma W and Mayr C 2018 A membraneless organelle associated with the endoplasmic reticulum enables 3' UTR-mediated protein-protein interactions. *Cell* **175** 1492–1506

Milovanovic D, Wu Y, Bian X and De Camilli P 2018 A liquid phase of synapsin and lipid vesicles. *Science* **361** 604–607

Mitrea DM and Kriwacki RW 2016 Phase separation in biology, functional organization of a higher order. *Cell Commun. Signal*

Nigg PE and Pavlovic J 2015 Oligomerization and GTP-binding Requirements of MxA for viral target recognition and antiviral activity against Influenza A Virus. *J. Biol. Chem.* **290** 29893–29906

Rai AK, Chen JX, Selbach M and Pelkmans L 2018 Kinase-controlled phase transition of membraneless organelles in mitosis. *Nature* **559** 211–216

Sabari BR, Dall'Agnese A, Boija A, Klein IA, Coffey EL, *et al*. 2018 Coactivator condensation at super-enhancers links phase separation and gene control. *Science*

Sadler AJ and Williams B 2011 Dynamiting viruses with MxA. *Immunity* **35** 491–493

Sehgal PB 2019 Biomolecular condensates in cancer cell biology: interleukin-6- induced cytoplasmic and nuclear STAT3/PY-STAT3 condensates in hepatoma cells. *Contemp. Oncol. (pozn)* **23** 16–22

Sehgal PB, Westley J, Lerea KM, DiSenso-Browne S and Etlinger JD 2020 Biomolecular condensates in cell biology and virology: phase-separated membraneless organelles (MLOs). *Anal. Biochem.* **597** 113691

Sehgal PB, Yuan H, Scott MF, Deng Y, Liang FX, *et al*. 2020 Murine GFP-Mx1 forms phase-separated nuclear condensates and associates with cytoplasmic intermediate filaments: novel antiviral activity against vesicular stomatitis virus. *J. Biol. Chem.* **597** 113691

Shiina N 2019 Liquid- and solid-like RNA granules form through specific scaffold proteins and combine into biphasic granules. *J. Biol Chem.* **294** 3532–3548

Shin Y and Brangwynne CP 2017 Liquid phase condensation in cell physiology and disease. *Science* **357** eaaf4382

Shirodkar MV 1965 The blocking effect of West Nile virus on production of sarcoma by Rous virus in chickens. *J. Immunol.* **95** 1121–1128

Steiner F and Pavlovic J 2020 Subcellular localization of MxB determines its antiviral potential against influenza virus. *J. Virol.* **94** e00125-e220

Stertz S, Reichelt M, Krunse-Locker J, Mackenzie J, Simpson JC, Haller O and Kochs G 2006 Interferon-induced, antiviral human MxA protein localizes to a distinct subcompartent of the smooth endoplasmic reticulum. *J. Interferon Cyt. Res.* **26** 650–660

Verhelst J, Hulpiau P and Saelens X 2013 Mx proteins: antiviral gatekeepers that restrain the uninvited. *Microbiol. Mol. Biol. Rev.* **77** 551–566

Yuan H and Sehgal PB 2016 MxA Is a novel regulator of endosome-associated transcriptional signaling by bone morphogenetic proteins 4 and 9 (BMP4 and BMP9). *PLoS One* **11** e0166382

Zürcher T, Pavlovic J and Staeheli P 1992a Nuclear localization of mouse Mx1 is necessary for inhibition of influenza virus. *J. Virol.* **66** 5059–5066

Zürcher T, Pavlovic J and Staeheli P 1992b Mechanism of human MxA protein action: variants with changed antiviral properties. *EMBO J.* **11** 1657–1661

Zürcher T, Pavlovic J and Staeheli P 1992c Mouse Mx2 protein inhibits vesicular stomatitis virus but not influenza virus. *Virology* **187** 796–800

Corresponding editor: KUNDAN SENGUPTA